Synchronization of Sound Sources

Markus Abel, Karsten Ahnert, and Steffen Bergweiler*

Department of Physics and Astronomy, Potsdam University, Karl-Liebknecht-Strasse 24, D-14476, Potsdam-Golm, Germany
(Received 17 April 2009; revised manuscript received 9 July 2009; published 9 September 2009)

Sound generation and interaction are highly complex, nonlinear, and self-organized. Nearly 150 years ago Rayleigh raised the following problem: two nearby organ pipes of different fundamental frequencies sound together almost inaudibly with identical pitch. This effect is now understood qualitatively by modern synchronization theory M. Abel *et al.* [J. Acoust. Soc. Am. **119**, 2467 (2006)]. For a detailed investigation, we substituted one pipe by an electric speaker. We observe that even minute driving signals force the pipe to synchronization, thus yielding three decades of synchronization—the largest range ever measured to our knowledge. Furthermore, a mutual silencing of the pipe is found, which can be explained by self-organized oscillations, of use for novel methods of noise abatement. Finally, we develop a reconstruction method which yields a perfect quantitative match of experiment and theory.

Introduction.—In a seminal publication Lord Rayleigh reported on experiments involving two organ pipes of close pitch, positioned next to each other. He observed the following peculiar behavior: alone, each pipe sounded with its own frequency; together they sounded in perfect unison and almost reduced one another to silence [1,2]. This phenomenon can be described by synchronization theory, a general nonlinear principle with striking applications in the natural sciences including physics, chemistry, neurology or biology [3].

Here, we focus on an organ pipe as (i) prototypical for aeroacoustical sound generation, (ii) paradigmatic for synchronization of coupled oscillators, and (iii) a beautiful musical instrument for which we present a mathematical model. By driving one organ pipe sinusoidally by an electric speaker we can demonstrate in great detail the importance of nonlinear effects in sound generation and interaction [4] in contrast to linear response theory [5] conventionally applied for musical instruments.

The general description of the dynamics of an organ pipe is given by the compressible Navier-Stokes equations with suitable boundary conditions. One can solve the equations numerically [6], or investigate them analytically [7]. Both ways reproduce different aspects of sound production. Here, we are interested in the *interaction* of an organ pipe with a sound source. Then, it is advantageous to model only the relevant characteristics in terms of reduced models [8]. Such an elementary model allowing for complex dynamics is given by an autonomous oscillator [3,9], which includes an oscillatory unit, energy supply, and energy loss by radiation and damping.

Let us identify these units in the organ pipe. Energy is supplied steadily by the wind system through the pipe foot and establishes a turbulent vortex street. Each time a vortex detaches, a pressure fluctuation enters the resonator, inside which characteristic waves are selected, and radiated at the pipe mouth by an oscillating air sheet [8,10]. In our model, this air sheet constitutes the basic oscillating unit. Inside the resonator sound pressure levels (SPLs) up to 160 dB can occur, such that viscous damping contributes in energy dissipation. External acoustical fields couple to the system through the air sheet, possibly described by a (nonlinear) acoustical admittance [11]. By Lighthills analogy [7], a coupling by the turbulent vortex street is expected to be of lower order.

The above scenario can be described by a reduced, two-dimensional model for the oscillatory unit ξ:

$$\ddot{\xi} - g(\xi, \dot{\xi}) = 0, \tag{1}$$

where the function $g(\xi, \dot{\xi})$ contains the above-mentioned ingredients and with the condition that a limit-cycle solution of frequency ν_0 exists. Then, with $\xi = A(t)e^{i\phi(t)}$ the phase ϕ and the amplitude A are well defined. An external driving enters on the right-hand side of Eq. (1). Corresponding to the experiment, sinusoidal driving is used: $\varepsilon \sin(2\pi\nu t + \phi_0)$ with ε the coupling strength. Here, one assumes that an oscillator represents the basic physics of the pipe with regard to sound generation and synchronization—typically, the oscillating air sheet [8]. Because the air sheet is the source of sound radiation, the measurement at the microphone can be taken as the state of the oscillator (with a phase shift accounting for distance).

Close to the limit cycle the amplitude is slaved by the phase, allowing the description in terms of the phase difference Ψ between driving and oscillator

$$\dot{\Psi} = -2\pi(\nu - \nu_0) + \varepsilon q(\Psi). \tag{2}$$

The parameters are driving frequency ν, and coupling ε. The study of the parameter plane (ν, ε) yields triangular-shaped synchronization regions, the well-known Arnold tongues [12].

In order to determine Eq. (1) *directly* from data, we have elaborated a numerical method based on embedding theory [13] which allows for a reconstruction and comparison of the characteristics of model and data. We recover the power spectra and synchronization properties of the organ

as an acoustical system. This opens the way for a detailed theoretical investigation of the system and hints to how a model can be derived from first principles.

The experiment.—The setup of the experiment is sketched in Fig. 1. The pipe [14] was wooden and closed at the upper end, tuned at $\nu_0 = 686$ Hz. It was driven by an especially fabricated miniature organ [14] with a blower connected to the wind belt and further by flexible tubes to the wind chest. Measurements took place inside a suitable anechoic box. The loudspeaker for the external, driving sound signal was positioned side-by-side to the organ pipe, cf. Fig. 1. The emitted signals were registered at a distance of 16 mm to either pipe and speaker, allowing for constructive or destructive interference of the superposed signals. To ensure that the phase of the pipe is correctly detected, we carried out simultaneous control measurements inside and outside the pipe and at the microphone—all results were consistent.

To explore the coupling-detuning plane (ν, ε), the loudspeaker SPL and frequency were varied separately, the first between $+10$ dB and -50 dB relative to the reference signal of the organ pipe in steps of 2 dB, the latter according to the size of the synchronization range. To determine the minimal achievable resolution in ν, we consider the sources of variations of the pipe's frequency. The wind pressure was 700 ± 9 Pa, giving a frequency variation of ± 0.1 Hz at the scale of seconds; the temperature varied with the circadian rhythm at 292 ± 1 K with a resulting variance of $\simeq 2$ Hz [15]. This slow change did not affect an individual run with a fixed SPL; however, runs with different SPLs were adjusted to the circadian variation. We measured the synchronization range down to the maximal resolution of 0.1 Hz as set by the wind supply; below noise destroys synchronization. With respect to noise, we enhanced the signal-to-noise ratio by long-time averaging, such that irregular phase slips are leveled out and a synchronization region can be obtained even for very small driving. This was achievable by heavily automatized measurements of a total duration of about 3 weeks.

We investigated two acoustically relevant characteristics: the frequency difference, $\Delta \nu / \nu_0 = (\nu_{speaker} - \nu_{pipe}) / \nu_0$, and the spectrum of the measured loudspeaker signal. Their dependence on the detuning is shown in Fig. 2 for two exemplary relative driving strengths, 0 and 10 dB. Note, that ν_{pipe} is the frequency of the *driven* pipe which might be different from its natural frequency.

The transition to synchronization can be seen from the graph for the frequency difference. For equal SPL and below (upper panel in Fig. 2), a saddle-node bifurcation is found, as predicted theoretically [3,16]. For couplings stronger than 0 dB, the bifurcation tends to become very sharp, indicating that the weakly nonlinear approximation [3] breaks down (lower panel Fig. 2).

In the graphs for the amplitude, one recognizes two effects: synchronization and resonance. Because of synchronization the phase shift between the two emitted signals varies within an interval of size π; as for Helmholtz resonance, the loudspeaker signal is phase shifted by $\sim \pi$ and reemitted by the pipe. From synchronization alone, the superposition of the signals of speaker and pipe can only vary within SPL$_{speaker} \pm$ SPL$_{pipe}$; with resonance much weaker amplitudes result, as seen in Fig. 2. This result implies a novel way of sound reduction, where the reductor acts as an active element, adjusting the frequency without any external control.
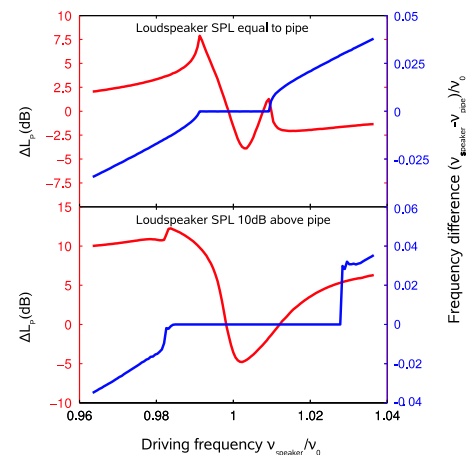
FIG. 2 (color online). Synchronization plot: if the detuning of pipe and loudspeaker is small enough, frequency synchronization is found as a plateau. Within the synchronization region, the phase difference Ψ varies over an interval of size π, where the measured SPL shows a sharp minimum for $\Psi = \pi$. Top (SPL$_{speaker}$ = SPL$_{pipe}$): the frequency shows a very nice plateau with a saddle-node bifurcation; for $\Psi = \pi$ negative interference is observed by a decrease of 6 dB. Bottom (SPL$_{speaker} \simeq$ SPL$_{pipe}$ + 10 dB): the transition from synchronization is quite sharp, indicating strong nonlinearities. The amplitude decrease can be explained by synchronization with an additional Helmholtz-resonator-like behavior of the pipe, deepening the SPL gap to 15 dB. The maximum is obtained by addition of the amplitudes to 12 dB.
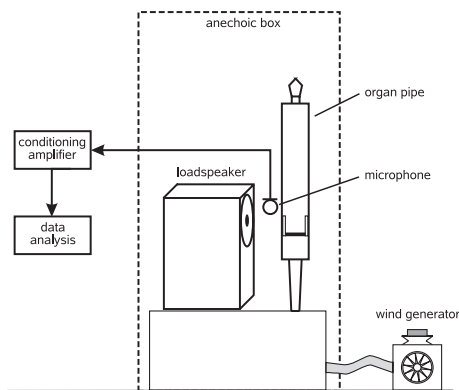

FIG. 1. Sketch of the experiment. Pipe and loudspeaker stand side by side, the signal is measured by a microphone with equal distance to both sound sources.

The full variation in parameter space is shown in the left panel of Fig. 3 by an Arnold tongue, here plotted logarithmically due to the enormous coupling range investigated. The color coding corresponds to the spectral power of the loudspeaker frequency $S(\nu_{\text{speaker}})$, measured at the microphone. We varied the amplitude of the loudspeaker from $+10$ dB to -50 dB, relative to the SPL of the organ pipe, in steps of 2 dB. The range covers 3 decades—the widest range ever measured in synchronization experiments. The synchronization edges are marked in Fig. 3 by white lines. Clearly, the linear shape is bent due to the semilog plotting.

Reconstruction of the dynamical system.—We do not have access to the "state" of the oscillating air sheet, but we know the recorded SPL, $x(t)$, of the organ pipe. By embedding theory we can infer a differential embedding $(x, \dot{x}, \ddot{x}, \dots)$ with a maximal embedding dimension of three [13,17]. In this space there exists an equivalent to Eq. (1): $\ddot{x} - f(x, \dot{x}) = 0$. We reconstruct this equation step by step to further investigate its dynamical and predictive properties.

The data series consists of 110250 data points, with a sampling rate of 11 025 Hz. Normalization in space and time yields variance 0.5 and frequency 1. The crucial computation of derivatives was accomplished by spectral smoothing [18]: (i) Fourier transformation, (ii) 8th order Butterworth filtering with cutoff at $4.5\nu_0$ to suppress noise amplification, and (iii) backtransformation. If the cutoff is increased more harmonics enter the filtered time series; if the cutoff is too low too much information is filtered out;

i.e., the necessary nonlinearities are suppressed. Thorough testing yielded that in our case a three-dimensional embedding does not improve the results.

The unknown function f is estimated by nonparametric regression, formulated as a minimization problem: $\|\ddot{x} - f(x, \dot{x})\|_2 \overset{!}{=} \min$, with $\|\cdot\|_2$ the l^2 norm of the data vector. The unknown function f is found by variation in function space, where we used, for the sake of computational simplicity, polynomials of order three [19,20]; higher orders do not improve the model. Specifically, $f(x, \dot{x}) = a_0 + a_1 x + a_2 x^2 + a_3 x^3 + a_4 \dot{x} + a_5 \dot{x}^2 + a_6 \dot{x}^3 + a_7 x\dot{x} + a_8 x^2 \dot{x} + a_9 x\dot{x}^2$ with $a_0 = 0.25$, $a_1 = -0.92$, $a_2 = -0.18$, $a_3 = -0.12$, $a_4 = 0.20$, $a_5 = -0.33$, $a_6 = 0.056$, $a_7 = -0.015$, $a_8 = -0.923$, $a_9 = -0.072$. Note the striking similarity to the van der Pol oscillator with $f_{\text{vdP}} = -x + \dot{x}(1 - x^2)$, reflected in the dominant coefficients a_1 and a_8. The latter is responsible for nonlinear damping, whereas energy is supplied by the constant and the $\dot{x}$ term. Other terms assist nonlinear damping and are indispensable to find the correct frequencies in the reconstructed system. Since the observables are not directly related to the physical driving (wind) and damping mechanisms we hesitate to give a complete physical interpretation.

Numerical stability analysis yields a repelling fixed point at (0.254,0) and an attracting limit cycle, plotted in the inset of Fig. 4, which shows convincing coincidence with the filtered experimental data. For acoustical comparison, we compare the power spectra of pipe and reconstruction in Fig. 4. The positions of the harmonics are in perfect agreement, and their ratio coincides well.

Finally, the model is synchronized with an external, sinusoidal driving. For the coupled equation, we solve $\ddot{x} = f(x, \dot{x}) + \epsilon \sin(\omega t)$, with the driving frequency ω and the coupling parameter $\epsilon = 0.025 \text{SPL}_{\text{speaker}}$. The latter relation describes the influence of the loudspeaker on the pipe with a factor 0.025, determined in order to obtain optimal coincidence of experimental and reconstructed Arnold tongue, see Fig. 3. Recently, a way to extract the coupling from data has been proposed [21]; in principle it can be obtained by a detailed analysis of acoustics and fluid dynamics at the pipe mouth.

Conclusion.—Since the time of Lord Rayleigh the nonlinear interaction of acoustical sources has been under discussion [1]. We highlight the acoustical effects of phase synchronization, experimentally realized by an organ pipe driven externally by a loudspeaker. The application of synchronization theory suggests a novel type of sound control, where the passive element adjusts its frequency *exactly* to the source. Since the system involved can be abstracted, we conclude that such a control can be applied to a diversity of situations, from musical instruments to noise reduction in vibrating systems, be it mechanical or hydromechanical.

With respect to synchronization, we found the deepest Arnold tongue ever seen experimentally, suggesting wind
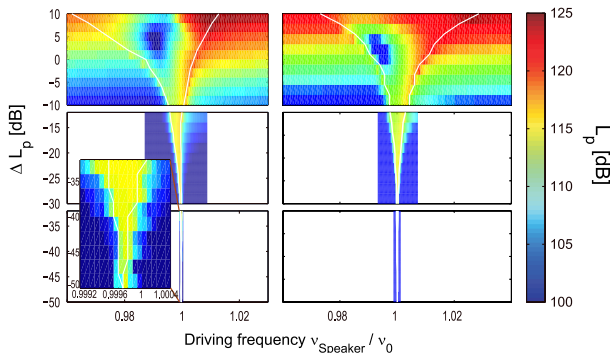

FIG. 3 (color online). Arnold tongue measured over approximately 3 decades. The left plot shows the tongue obtained from the experimental data, while the right one shows the reconstructed tongue. The color coding corresponds to the amplitude measured at the microphone position at the loudspeaker frequency $S(\nu_{\text{speaker}})$. To guide the eye, the synchronization region is marked by a straight line. The synchronization edge grows linearly with the coupling, seen as a logarithmic bend in the used semilog plot. The lowest possible frequency resolution, 0.1 Hz, corresponds to the variation of the frequency produced by the wind supply, shown by the inset. The reconstructed Arnold tongue is much more symmetric. This indicates again strong nonlinearities. The coincidence between experiment and model is almost perfect in the low-coupling region.
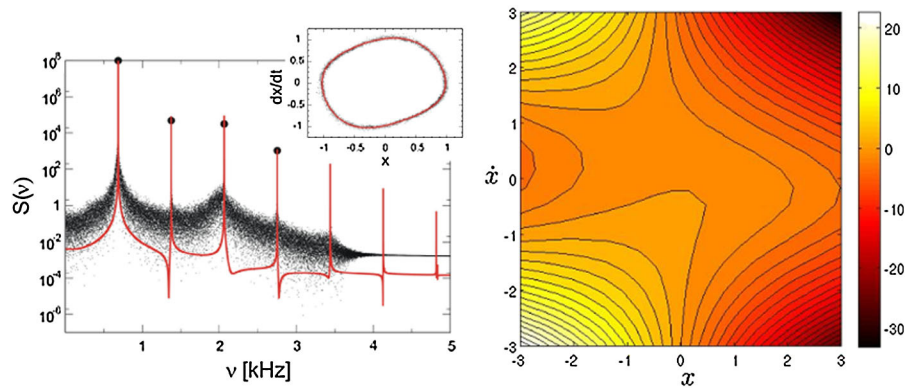
FIG. 4 (color online).   Left: The power spectra of the measured (black) and the reconstructed signal (gray). The musical sound is reproduced quite nicely, as recognized by the coincidence of the spectra; for better visibility the maxima of the measured signal are shown by black dots. The inset shows the time series and its reconstruction in the embedding space, which coincide very well. Right: Contour plot of the function f found by nonparametric regression, the color coding is shown by the colorbar on the right.

instruments as paradigmatic for synchronization. The results confirm the theory for small coupling; for large coupling we give experimental access to nonlinear correction terms to be analyzed further. To analyze the acoustical properties of the pipe we propose an autonomous oscillator, reconstructed from a novel type of data analysis. The agreement between model and experiment in terms of Arnold tongues and power spectra is excellent—musical and synchronization characteristics are well reproduced. Conventional methods, as transfer functions, or admittance [22] do not allow such a direct interpretation.

In this Letter acoustics is paired with nonlinear dynamics and data mining. Organ builders have developed complicated empirical rules to arrange organ pipes within a register to avoid synchronization effects. Our results do not only allow for an easy simulation of instruments, but as well development cycles and tuning of instruments could be enhanced. Noise reduction is possible by self-organization of two sound sources such that they interfere negatively—no external control is needed. The applications of this principle might be interesting for a variety of technically important situations.

We acknowledge inspiring discussion with A. Pikovsky and M. Rosenblum, and thank F. Spahn for many suggestions. The organ builder company Schuke GmbH constructed the pipes and the wind supply system.

*Corresponding author.
markus.abel@physik.uni-potsdam.de
[1] J. Rayleigh, *The Theory of Sound* (Dover, New York, 1945).
[2] http://www.stat.physik.uni-potsdam.de/~organ/
[3] A. Pikovsky, M. Rosenblum, and J. Kurths, *Synchronization—A Universal Concept in Nonlinear Science* (Springer, Berlin, 2001).
[4] N. H. Fletcher, Rep. Prog. Phys. **62**, 723 (1999); J. Acoust. Soc. Am. **64**, 1566 (1978).
[5] T. Rossing and N. Fletcher, *The Physics of Musical Instruments* (Springer, New York, 1998).
[6] S. Succi, *The Lattice Boltzmann Equation for Fluid Dynamics and Beyond* (Oxford University Press, New York, 2001); J. C. Hardin and M. Y. Hussaini, *Computational Aeroacoustics* (Springer, Berlin, 1993).
[7] M. S. Howe, *Theory of Vortex Sound*, Cambridge Texts in Applied Mathematics (Cambridge University Press, Cambridge, U.K., 2003).
[8] B. Fabre and A. Hirschberg, Acust. Acta Acust. **86**, 599 (2000).
[9] A. Nayfeh and D. Mook, *Nonlinear Oscillations* (John Wiley, New York, 1979).
[10] B. Fabre, A. Hirschberg, and A. P. J. Wijnands, Acust. Acta Acust. **82**, 863 (1996).
[11] S. Thwaites and N. H. Fletcher, J. Acoust. Soc. Am. **74**, 400 (1983).
[12] V. I. Arnold, Chaos **1**, 20 (1991).
[13] T. Sauer, J. Yorke, and M. Casdagli, J. Stat. Phys. **65**, 579 (1991).
[14] Alexander Schuke GmbH, 2004, http://www.schuke.com.
[15] D. A. Bohn, J. Audio Eng. Soc. **36**, 223 (1988).
[16] M. Abel, S. Bergweiler, and R. Gerhard-Multhaupt, J. Acoust. Soc. Am. **119**, 2467 (2006).
[17] N. B. Tufillaro, P. Wyckoff, R. Brown, T. Schreiber, and T. Molteno, Phys. Rev. E **51**, 164 (1995).
[18] K. Ahnert and M. Abel, Comput. Phys. Commun. **177**, 764 (2007).
[19] M. Abel, K. Ahnert, S. Mandelj, and J. Kurths, Phys. Rev. E **71**, 015203 (2005).
[20] G. Gouesbet and C. Letellier, Phys. Rev. E **49**, 4955 (1994).
[21] B. Kralemann, L. Cimponeriu, M. G. Rosenblum, A. S. Pikovsky, and R. Mrowka, Phys. Rev. E **77**, 066205 (2008).
[22] T. Cox and P. D'Antonio, *Acoustic Diffusers and Absorbers: Theory, Design and Application* (Taylor & Francis, London, 2004).